

doi:10.15199/48.2023.03.26

## Design of suspension control system for bearingless induction motor using self tuning fuzzy-PID controller

**Abstract.** A bearingless induction motor (BIM) has many advantages, resulting in fast growing interest in this motor. BIM combines the functions of both torque generation and magnetic suspension, the essential requirements for controlling the (BIM) is to generate an electromagnetic force that makes the rotor rotates within a certain limit at the centre of the stator, and this must be maintained even when the motor is exposed to internal disturbances like variation of speed or external disturbance like applying forces on the rotor shaft. This paper proposed a design and simulation of suspension control system for a bearingless induction motor by using on-line self tuning fuzzy-PID methods. The proposed controller provides better performance than the traditional PID, the results show that the fuzzy-PID controller reduces the rotor deviation by 36% under effect of external disturbance force and by 66.7% under effect of speed variation.

**Streszczenie.** Bezłożyskowy silnik indukcyjny (BIM) ma wiele zalet, co skutkuje szybko rosnącym zainteresowaniem tym silnikiem. BIM łączy w sobie funkcje generowania momentu obrotowego i zawieszenia magnetycznego, podstawowe wymagania dotyczące sterowania (BIM) to generowanie siły elektromagnetycznej, która powoduje, że wirnik obraca się w pewnym zakresie w środku stojana i musi to być utrzymywane nawet wtedy, gdy silnik jest narażony na zakłócenia wewnętrzne, takie jak zmiany prędkości lub zakłócenia zewnętrzne, takie jak przykładanie sił do wału wirnika. W artykule zaproponowano zaprojektowanie i symulację układu sterowania zawieszeniem bezłożyskowego silnika indukcyjnego z wykorzystaniem metod samostrojenia rozmytego PID on-line. Zaproponowany regulator zapewnia lepsze osiągi niż tradycyjny PID, wyniki pokazują, że regulator rozmyty PID zmniejsza odchylenie wirnika o 36% pod wpływem zewnętrznej siły zakłócającej o 66,7% pod wpływem zmian prędkości. (Projekt układu sterowania zawieszeniem bezłożyskowego silnika indukcyjnego z wykorzystaniem samostrojącego regulatora rozmytego PID)

**Keywords:** Bearingless induction motor, Suspension force, Self tuning fuzzy PID, Flux oriented control

**Słowa kluczowe:** Bezłożyskowy silnik indukcyjny, siła zawieszenia, Samostrojenie rozmyte PID, kontrola zorientowana na strumień

### Introduction

A magnetic bearing motor is a no-contact bearing between both the stator and the rotor by electromagnetic radial force, which solves the problems of motor like as wear, noise, vibration and lubrication [1], [2]. Therefore, this type of machines is applied in special devices such as air compressors, mechanical heart pumps, and mechanical blood injectors. But, the magnetic bearing machine has a large overall length, and a difficult construction. Bearingless induction motors, are the suitable solution for magnetic bearing limitations, which combine the magnetic bearing and the traditional motor, that use their own windings to generate electromagnetic attraction forces that make the rotor centred [3]–[5]. A novel motor is considered as a bearingless motor that produces the radial suspension force and the rotation torque which its depend on the break of the uniformity of the air-gap magnetization, using the unequal pole-pair coils as two sets are installed in stator of the bearingless induction motor that generates rotational torque and axial levitations force and performs rotor rotation and suspension forces [6]–[8]. When compared to other modes of bearingless motor, the bearingless induction motor not only has the advantages of a traditional induction motor, including an easy structure, minimal pulsating of torque, and simple flux weakening regulation, it also has the benefits of a magnetic bearing, including no touch, no erosion, no pollution, and a length of service life [8].

The important problems and requirements for controlling the (BIM) is to generate an electromagnetic force that makes the rotor rotates at the center of stator bore to avoid the rotor from colliding with the stator. An active disturbances rejection control (ADRC) system for a bearingless induction motor was proposed [9], the simulation results of this controller (ADRC) can improve the performance of the dynamic control. The radial position control by using Fuzzy Controller for a BIM has been proposed in [10], The results of this control system confirmed the best performance at operating point and at steady state. Also sliding mode with variable structure of

Bearingless Motor (SMVS) has been proposed by [11] to realize high performance dynamic control and successfully counteract the effects of the motor parameters change and the load disturbance.

The problem of the conventional PID controller it is impacted by the changing of motor parameters and load disturbance. in order to solve the problem of the conventional PID, the controller that proposed in this paper is based on self tuning fuzzy PID.

The objective of this paper is to find the optimal parameters of PID on-line to improve the control performance and achieve high stability for the system even if it is exposed to external disturbance, as well as changes in load and speed.

### Mathematical model of a bearingless induction motor

A bearingless induction motor includes, two sets of windings are imbedded in the stator, four-poles rotation torque windings to generates the rotation torque and two poles suspension control winding to generates the levitation force as shown in Fig.1, therefore the mathematical representation of the (BIM) is divided into two parts, electromagnetic torque model and axial levitation Force model.

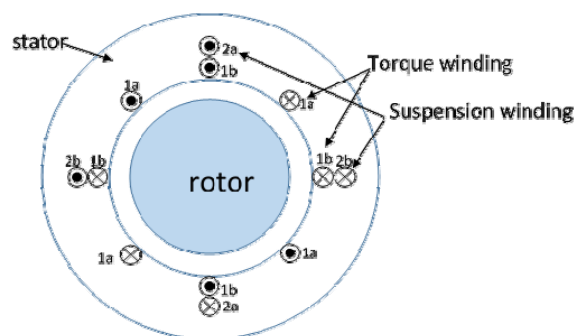


Fig.1. Structure of bearing less induction motor

### Electromagnetic torque model

Because of the magnetic field of radial suspension winding is very small with respect to the magnetic field of the torque winding, it can be ignored, so we can write the equation of the air-gap flux linkage in the dq coordinates of the torque winding as [12]–[15]:

$$(1) \quad \psi_{1d} = L_{1m} (i_{1sd} + i_{1rd})$$

$$(2) \quad \psi_{1q} = L_{1m} (i_{1sq} + i_{1rq})$$

Where:  $i_{1sd}$ ,  $i_{1sq}$ ,  $i_{1rd}$  and  $i_{1rq}$  - stator and rotor current components of electromagnetic torque windings in  $d$ - $q$  coordinate, respectively,  $L_{1m}$  is the mutual inductance of electromagnetic torque winding. The electromagnetic torque equation can be written as:

$$(3) \quad Te = P_1 (i_{1sq} \psi_{1d} - i_{1sd} \psi_{1q})$$

Where:  $P_1$  – number of poles for torque windings.

### Axial levitation Force Model

In this section, by using the air-gap flux distributions to derive the inductance matrix, some elements of this matrix are a function of the radial rotor displacement. Let us assume that the flux linkages of windings 1a, 1b, 2a and 2b are  $\psi_{1a}$ ,  $\psi_{1b}$ ,  $\psi_{2a}$  and  $\psi_{2b}$ , respectively and the instantaneous currents of windings 1a, 1b, 2a and 2b are  $i_{1a}$ ,  $i_{1b}$ ,  $i_{2a}$  and  $i_{2b}$  respectively. The relationships of The flux linkage and current may be expressed as [16]– [20]:

$$(4) \quad [\psi] = [L] * [i]$$

$$(5) \quad \begin{bmatrix} \psi_{1a} \\ \psi_{1b} \\ \psi_{2a} \\ \psi_{2b} \end{bmatrix} = \begin{bmatrix} L_{1a} & M_{1a1b} & M_{1a2a} & M_{1a2b} \\ M_{1b1a} & L_{1b} & M_{1b2a} & M_{1b2b} \\ M_{2a1a} & M_{2a1b} & L_{2a} & M_{2a2b} \\ M_{2b1a} & M_{2b1b} & M_{2b2a} & L_{2b} \end{bmatrix} * \begin{bmatrix} i_{1a} \\ i_{1b} \\ i_{2a} \\ i_{2b} \end{bmatrix}$$

Where  $L$  and  $M$  - self and mutual inductance respectively. Subscript 1 and Subscript 2 represent torque and suspension winding respectively.

$$(6) \quad \begin{bmatrix} M_{1a2a} & M_{1a2b} \\ M_{1b2a} & M_{1b2b} \end{bmatrix} = \tilde{M} \begin{bmatrix} -X & Y \\ Y & X \end{bmatrix}$$

$$(7) \quad L_{1a} = L_{1b} = \frac{\pi \mu_0 r \ell N_1^2}{4 g_0}$$

$$(8) \quad L_{2a} = L_{2b} = \frac{\pi \mu_0 r \ell N_2^2}{4 g_0}$$

$$(9) \quad M_{1a1b} = M_{1b1a} = M_{2a2b} = M_{2b2a} = 0$$

$$(10) \quad \tilde{M} = \frac{\pi \mu_0 r \ell N_1 N_2}{8 g_0} \quad \text{then}$$

$$(11) \quad [L] = \begin{bmatrix} L_1 & 0 & -\tilde{M}X & \tilde{M}Y \\ 0 & L_1 & \tilde{M}Y & \tilde{M}X \\ -\tilde{M}X & \tilde{M}Y & L_2 & 0 \\ \tilde{M}Y & \tilde{M}X & 0 & L_2 \end{bmatrix}$$

The transfer matrix equation of currents is:

$$(12) \quad [i]^T = [i_{1a} \quad i_{1b} \quad i_{2a} \quad i_{2b}]$$

The magnetic energy ( $W$ ) which is stored in a bearingless machine derives from the relationship of inductance form  $[L]$ , assuming linear electromagnetic networks as shown below:

$$(13) \quad [W] = \frac{1}{2} [i]^T * [L] * [i]$$

Then, the axial forces  $F_x$  and  $F_y$  in the two directions may be expressed as:

$$(14) \quad \begin{bmatrix} F_x \\ F_y \end{bmatrix} = \left[ \frac{dW}{dx} \right] = \tilde{M} * \begin{bmatrix} -i_{1a} & i_{1b} \\ i_{1b} & i_{1a} \end{bmatrix} * \begin{bmatrix} i_{2a} \\ i_{2b} \end{bmatrix}$$

Let  $i_{1a} = I_m \cos(\omega t)$ ,  $i_{1b} = I_m \sin(\omega t)$

$$(15) \quad \begin{bmatrix} F_x \\ F_y \end{bmatrix} = \tilde{M} * I_m \begin{bmatrix} -\cos(\omega t) & \sin(\omega t) \\ \sin(\omega t) & \cos(\omega t) \end{bmatrix} * \begin{bmatrix} i_{2a}^* \\ i_{2b}^* \end{bmatrix}$$

### The linear motion equation of the BIM suspended rotor

Depending on the Newton second law, the linear motion equations for the rotor as shown in Fig. 2 are expressed as [13], [15], [21]–[23]:

$$(16) \quad F_x + F_{sx} + F_{dx} = m \ddot{X}$$

$$(17) \quad F_y + F_{sy} + F_{dy} = m \ddot{Y}$$

Where:  $F_{sx} = K_s X$ ,  $F_{sy} = K_s Y$ ,

$$(18) \quad K_s = 0.3 \frac{r \ell \pi B^2}{\mu_0 g}$$

Where:  $m$  - mass of the rotor,  $F_{sx}$  and  $F_{sy}$  - unbalanced magnetic forces in X and Y-axis respectively,  $F_{dx}$ ,  $F_{dy}$  - the effect of the external disturbance and weight of rotor in X and Y-axis respectively,  $k_s$  - radial displacement factor,  $g$  - length of air gap,  $\mu_0$  - vacuum permeability,  $r, \ell$  - radius and long of the rotor respectively,  $B$  - flux density.

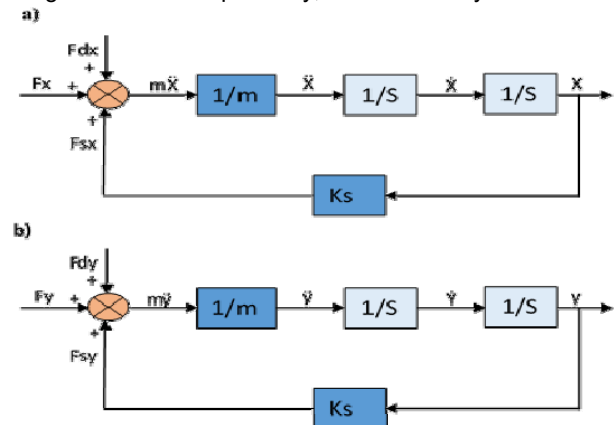


Fig.1. State space representation of rotor motion in (a) X direction (b) Y direction

### Speed of BIM

The working principle of vector control (field-oriented control) of a three phase induction motor enables us to deal with the three phase induction motor as a separately excited DC-motor. So the torque and flux can be controlled separately. The performance vector control in case of three-phase IM can be solved by the complex equations. The three-phase stationary system(abc) firstly, transformed to two-phase stationary ( $\alpha\beta$ ), and then transformed to rotating



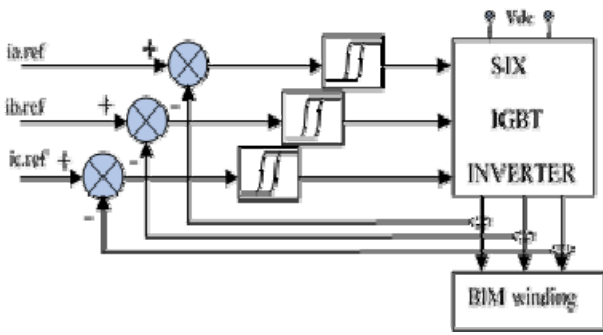


Fig. 4 Three phase inverter with hysteresis current controller

Table 1. parameters of the BIM.

symbols	value	discretion
Lm1	0.1586	mutual inductance of torque windings (H)
L1r	0.0092	leakage inductance of rotor (H)
R1r	11.48	Rotor resistance ( $\Omega$ )
J	0.00796	Moment of inertia (Kg.m <sup>2</sup> )
l	105	Long of rotor (mm)
r	97.8	diameter of rotor (mm)
m	2.86	Mass of rotor (Kg)
N1	60	No. of turn of torque winding
N2	140	No. of turn of suspension winding
P1	2	Pole pairs of torque winding
P2	1	Pole pairs of torque winding
g	0.6	Air-gab (mm)

### Suspension force control

In BIM, there is a new group of windings was added with the main winding. The advantage of this winding is to make the rotor rotates in the center of the stator and prevent it from colliding with the stator, which is controlled by an external control system.

PID control system is one of the most widely used control units in industrial fields, it contains three main parts: proportional (P) integral (I) derivative (D), that can be shown in Fig. 5. The output of the PID control system (U) is expressed as[26]:

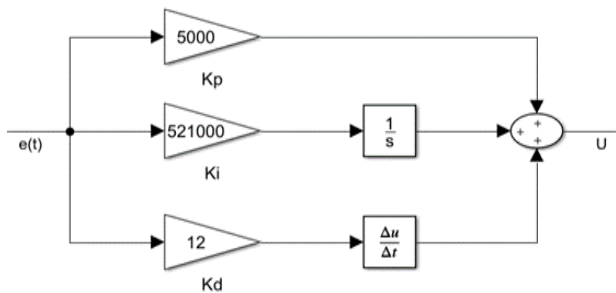


Fig. 5. Simulation model of PID Controller

$$(28) \quad U = Kp e(t) + Ki \int e(t) + Kd \frac{de}{dt}$$

By using ziguler method to calculate Kp, Ki, Kd

At  $K_{cr} = 8333$ ,  $P_{cr} = 19.2$  ms then.

Where:  $P_{cr} = 1/T_{cr}$ ,  $K_{cr}$  is critical gain,  $T_{cr}$  is critical time. From ziguler method table.

$Kp = 5000$ ,  $Ki = 521000$ ,  $Kd = 12$

In order to solving the problems that conventional PID controller is impacted by the changing of motor parameters and load disturbance the self tuning fuzzy PID controller is

proposed as shown in Fig. 6. The values of Kp1, Ki1, Kd1 are adjusted on-line by using fuzzification, fuzzy rule and defuzzification of both of error E and the change of error EC, since the controller parameters will be change with change of E and EC on line, fuzzy PID controller is used in suspension force controller instead of traditional PID controller[26]–[31].

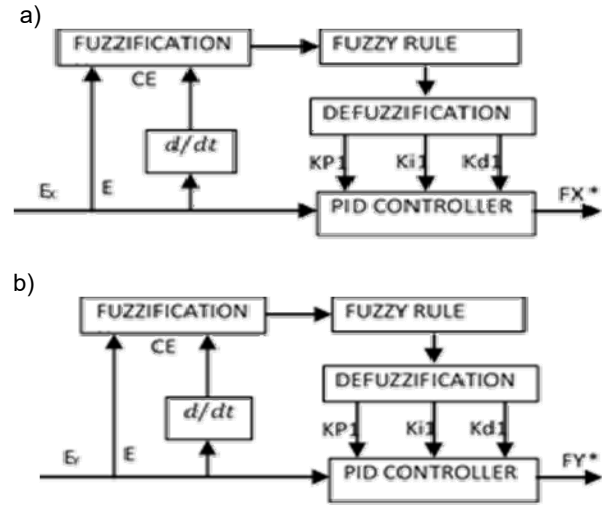


Fig. 6. Structure of fuzzy PID control system (a) X-axis (b) Y-axis

Fig. 7 shows the simulation of the self tuning fuzzy PID control system. the overall equations of the parameters for the controller are:

$$(29) \quad Kp2 = Kp1 * Kp$$

$$(30) \quad Ki2 = Ki1 * Ki$$

$$(31) \quad Kd2 = Kd1 * Kd$$

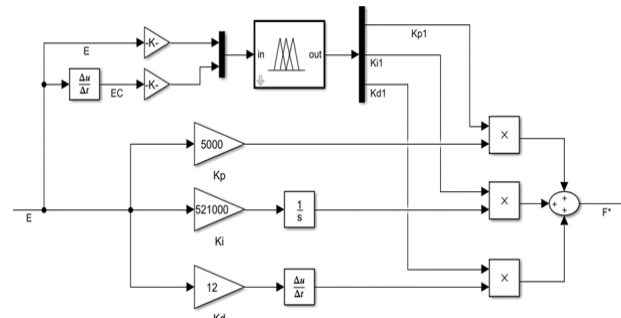


Fig. 7 Simulation of the self tuning fuzzy PID controller

Fuzzy controller that used in this paper has two inputs, displacement error and the change of error, and three outputs to determine the value of Kp1, Ki1 and Kd1. There is a membership function for each one of inputs and outputs. The inputs of fuzzy controller are the error (E) and the change of error (EC). NB, NS, Z, PS and PB (negative big, negative small, zero, positive small and positive big) respectively are input and lingual variables, where Their universe of (E) and (EC) is [-1 1] as shown in Fig. 8. There are six types of membership functions like triangle, trapezoidal, sigmoidal, Gaussian, z-type and s-type function. In this paper the shape of membership functions was selected as triangle for each input and output that gives the most accurate results than other types of membership functions.

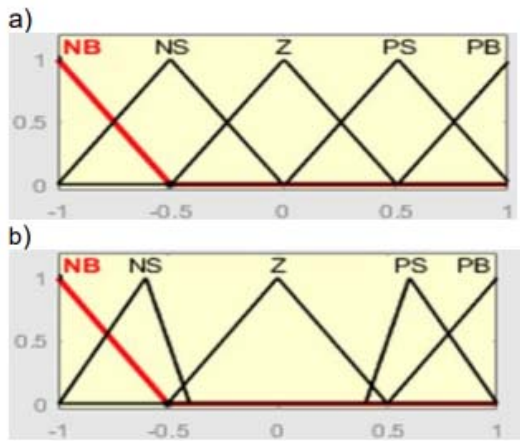


Fig. 8. Input membership function of (a) error (E), (b) change of error (EC)

The outputs are  $K_p1$ ,  $K_i1$  and  $k_d1$ , output lingual variables are Z, S, M and L (zero, small, medium and large) and their universe of [1 2.5], this universe (range) limits the amount of increment in PID parameters. The shape of membership function for each  $K_p1$ ,  $K_i1$  and  $k_d1$  as shown in Fig. 9.

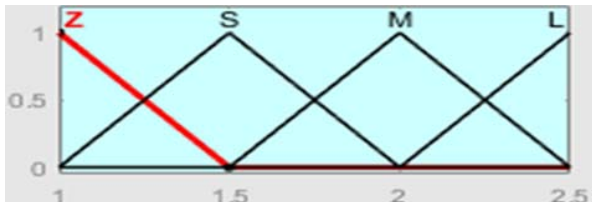


Fig. 9. Output membership functions of  $K_p1$ ,  $K_i1$ ,  $K_d1$

The system rules were varied until they couldn't improve the response of the system. Then the rules of fuzzy controller for  $K_p1$ ,  $K_i1$  and  $k_d1$  are presented in Table 2.

Table 2. Fuzzy rule of (a)  $K_p1$  and  $K_i1$  (b)  $K_d1$

a)

E \ EC	NB	NS	Z	PS	PB
NB	L	L	M	S	Z
NS	L	M	S	Z	M
Z	M	S	Z	S	M
PS	S	Z	S	M	L
PB	Z	S	M	L	L

b)

E \ EC	NB	NS	Z	PS	PB
NB	M	M	S	S	Z
NS	M	S	Z	Z	S
Z	S	Z	Z	Z	S
PS	S	Z	Z	S	M
PB	Z	S	S	M	M

### Results of simulation

In order to validate the proposed control strategy, the BIM model is subjected to various operating conditions, initially, the motor is operated at 3400 rpm with  $T_L=6$  Nm and without any external disturbance force on the rotor. At time 0.3 s, an external disturbance force of (50N) toward the negative X axis direction is applied on the rotor, and then at time 0.5s, this disturbance force is removed. Fig. 10a shows the external disturbance force, at time 0.3s the suspension force  $F_x$  will increase from 0 to 50N with 44% overshoot by using traditional PID, the overshoots decreased to 28% by using proposed fuzzy PID, at time

0.5s the suspension force ( $F_x$ ) will decrease to 0 because the external force was removed, Fig. 10b shows the variation of  $F_x$ . Fig.10c shows the deviation of the rotor from the centre in X direction, at time 0.3s, the peak-to-peak value of deviation is  $25\mu\text{m}$  by using traditional PID and  $9\mu\text{m}$  by the proposed fuzzy PID, at time 0.5s, the same effect will occur on the position of the rotor but in the opposite direction. Fig.10d shows the current of the suspension windings, before disturbance the three-phase suspension current is 75 mA to face the weight of rotor and then the current increases to 164 mA at 0.3s to face both of the weight of the rotor and the external force.

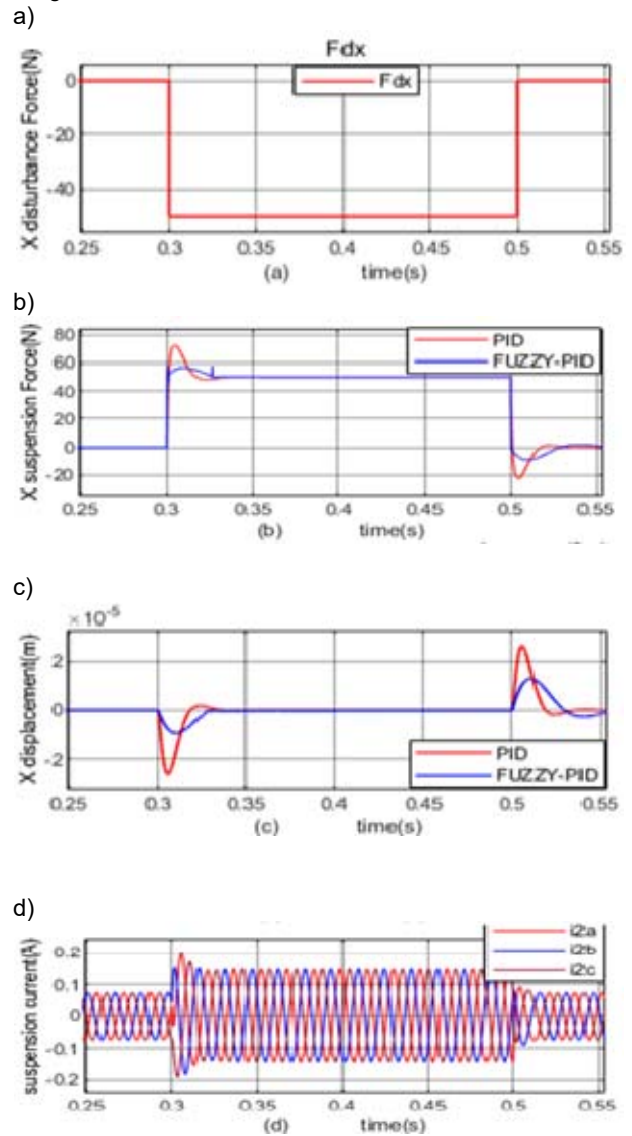


Fig. 10. Effect of external force disturbance (a) x disturbance force (b) suspension force (c) X displacement (d) suspension current

Fig.11a shows the variation of the reference speed which applied to the rotor to evaluate the performance of the suspension control system during internal disturbance at time 0.4s the reference speed ( $\omega^*$ ) increase from 3440 to 4060 rpm (360 to 425 rad/s). The rotor speed ( $\omega_r$ ) will rise to steady state at 36 ms, Fig.11b shows at time 0.4s the effect of speed change on the rotor displacement in X direction, the peak to peak value of vibration displacement is  $21\mu\text{m}$  with conventional PID this displacement will decrease to  $14\mu\text{m}$  with proposed fuzzy PID. Fig.11c shows at time 0.4s the effect of speed change on the rotor

displacement in Y direction, the peak to peak value of vibration displacement is 13  $\mu\text{m}$  with conventional PID this displacement will decrease to 9  $\mu\text{m}$  with proposed fuzzy PID. Fig.11d shows the effect of change the speed on suspension current, when the torque current grows up with the increase of speed the suspension current will slow down because the suspension force depends on all of the torque current ( $i_{1q}$ ) and suspension current. the suspension current return to normal value when the speed arrives to the steady state.

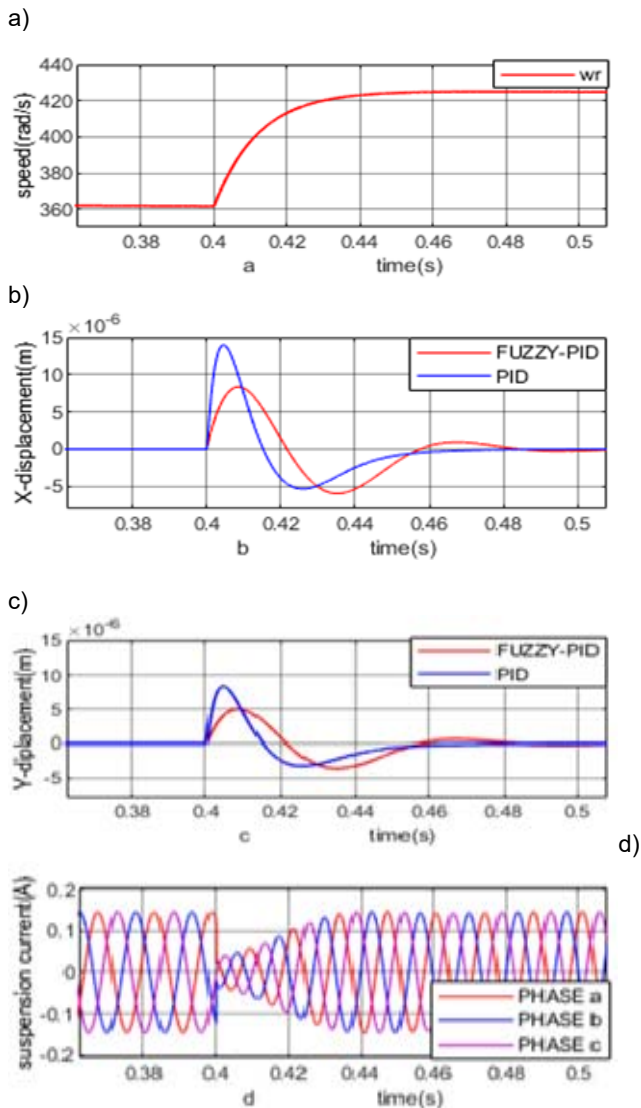


Fig. 11. Effect of speed change(a) rotor speed (b) X axis displacement (c) Y axis displacement (d) suspension current

## Conclusion

Non-linearity characteristics of the BIM, and the effect of some unknown elements such as external disturbance force and the change of speed, the traditional PID controller could not achieve optimal control performance. This work proposed on line self tuning fuzzy-PID controller for tuning PID parameters. This system has advantages of simple constructor and high flexibility. From the results of simulation by using the proposed control system, the peak to peak vibration of rotor position (displacement) decreases to 36% with external disturbance and it decreases to 66.7% with speed change. the simulation results of this controller demonstrated that the proposed system is very feasible of the BIM.

## Authors:

Qasim K Jasim He received a Bachelor's degree in Electrical Engineering from Babylon University, Iraq. He is currently studying toward a Master's degree of Science in Electrical Power Engineering at the University of Technology, Iraq.  
Email: eee.20.70@grad.uotechnology.edu.iq.  
Asst. Prof Dr. Mohammed Moanes E. Ali, Department of Electrical Engineering, University of Technology, Iraq. Mohammed Moanes published more than twenty-four technical papers.  
email: mohammedmoanes.e.ali@uotechnology.edu.iq

## REFERENCES

- [1] X. Ye, Z. Yang, J. Zhu, and Y. Guo, "Modeling and operation of a bearingless fixed-pole rotor induction motor," *IEEE Trans. Appl. Supercond.*, vol. 29, no. 2, Mar. 2019, doi: 10.1109/TASC.2018.2890382.
- [2] A. A. Yousif, A. M. Mohammed, and M. M. E. Ali, "Radial force cancellation of bearingless brushless direct current motor using integrated winding configuration," *Indones. J. Electr. Eng. Comput. Sci.*, vol. 25, no. 1, pp. 79–88, 2022.
- [3] N. Mamat, K. A. Karim, Z. Ibrahim, T. Sutikno, S. A. A. Tarusan, and A. Jidin, "Bearingless Permanent Magnet Synchronous Motor using Independent Control," *Int. J. Power Electron. Drive Syst.*, vol. 6, no. 2, pp. 233–241, 2015.
- [4] X. Ye and Z. Yang, "Development of Bearingless Induction Motors and Key Technologies," *IEEE Access*, vol. 7, pp. 121055–121066, 2019, doi: 10.1109/ACCESS.2019.2937118.
- [5] X. Ye, Z. Yang, J. Zhu, and Y. Guo, "Design and analysis of a bearingless fixed-pole rotor induction motor," in *2018 IEEE International Conference on Applied Superconductivity and Electromagnetic Devices (ASEMD)*, 2018, pp. 1–2.
- [6] X. Cao, J. Zhou, C. Liu, and Z. Deng, "Advanced control method for a single-winding bearingless switched reluctance motor to reduce torque ripple and radial displacement," *IEEE Trans. energy Convers.*, vol. 32, no. 4, pp. 1533–1543, 2017.
- [7] Z. Yang, D. Zhang, X. Sun, and X. Ye, "Adaptive exponential sliding mode control for a bearingless induction motor based on a disturbance observer," *IEEE Access*, vol. 6, pp. 35425–35434, 2018.
- [8] H. Zhu, Z. Yang, X. Sun, D. Wang, and X. Chen, "Rotor vibration control of a bearingless induction motor based on unbalanced force feed-forward compensation and current compensation," *IEEE Access*, vol. 8, pp. 12988–12998, 2020.
- [9] W.-S. Bu and Y.-Q. Huang, "Active disturbance rejection control of bearingless induction motor," in *international Conference on Electrical Engineering and Automation Control (ICEEAC)*, 2017, vol. 123, pp. 386–391.
- [10] E. A. D. F. Nunes *et al.*, "Proposal of a fuzzy controller for radial position in a bearingless induction motor," *IEEE Access*, vol. 7, pp. 114808–114816, 2019.
- [11] W. Bu, X. Zhang, and F. He, "Sliding mode variable structure control strategy of bearingless induction motor based on inverse system decoupling," *IEEE Trans. Electr. Electron. Eng.*, vol. 13, no. 7, pp. 1052–1059, 2018.
- [12] Z. Yang, Q. Ding, X. Sun, H. Zhu, and C. Lu, "Fractional-order sliding mode control for a bearingless induction motor based on improved load torque observer," *J. Franklin Inst.*, vol. 358, no. 7, pp. 3701–3725, 2021.
- [13] Z. Yang, K. Wang, X. Sun, and X. Ye, "Load disturbance rejection control of a bearingless induction motor based on fractional-order integral sliding mode," *Proc. Inst. Mech. Eng. Part I J. Syst. Control Eng.*, vol. 232, no. 10, pp. 1356–1364, 2018.
- [14] X. X. Liu, M. Y. Chen, X. Y. Shao, and Z. Q. Wang, "Study on Control System of Bearingless Induction Motor Based on Modified Internal Model Control," in *Advanced Materials Research*, 2011, vol. 317, pp. 567–572.
- [15] Z. Yang, D. Zhang, X. Sun, W. Sun, and L. Chen, "Nonsingular fast terminal sliding mode control for a bearingless induction motor," *IEEE Access*, vol. 5, pp. 16656–16664, 2017.
- [16] A. Chiba, T. Fukao, O. Ichikawa, M. Oshima, M. Takemoto, and D. G. Dorrell, *Magnetic bearings and bearingless drives*. Elsevier, 2005.
- [17] S. Nomura, A. Chiba, F. Nakamura, K. Ikeda, T. Fukao, and M. A. Rahman, "A radial position control of induction type bearingless motor considering phase delay caused by the rotor squirrel cage," in *Conference Record of the Power Conversion Conference-Yokohama 1993*, 1993, pp. 438–443.

- [18] A. Chiba, D. T. Power, and M. A. Rahman, "Analysis of no-load characteristics of a bearingless induction motor," *IEEE Trans. Ind. Appl.*, vol. 31, no. 1, pp. 77–83, 1995.
- [19] A. Chiba, R. Furuichi, Y. Aikawa, K. Shimada, Y. Takamoto, and T. Fukao, "Stable operation of induction-type bearingless motors under loaded conditions," *IEEE Trans. Ind. Appl.*, vol. 33, no. 4, pp. 919–924, 1997.
- [20] Q. Li and X. Liu, "Decoupling Control of Bearingless Induction Motor Based on Rotor Flux Orientation with Inverse System Theory," in *2010 International Conference on Measuring Technology and Mechatronics Automation*, 2010, vol. 1, pp. 894–897.
- [21] Z. Yang, J. Ji, X. Sun, H. Zhu, and Q. Zhao, "Active disturbance rejection control for bearingless induction motor based on hyperbolic tangent tracking differentiator," *IEEE J. Emerg. Sel. Top. Power Electron.*, vol. 8, no. 3, pp. 2623–2633, 2019.
- [22] Y. Chen, W. Bu, and Y. Qiao, "Research on the speed sliding mode observation method of a bearingless induction motor," *Energies*, vol. 14, no. 4, p. 864, 2021.
- [23] W. Bu, Y. Chen, and C. Zu, "Stator flux orientation inverse system decoupling control strategy of bearingless induction motor considering stator current dynamics," *IEEE Trans. Electr. Electron. Eng.*, vol. 14, no. 4, pp. 640–647, 2019.
- [24] C. X. Duan, Y. Han, and Y. H. Zhao, "Design of suspension control system for bearingless motor," in *Advanced Materials Research*, 2012, vol. 538, pp. 3277–3280.
- [25] I. Ferdiansyah, M. R. Rusli, B. Praharsena, H. Toar, and E. Purwanto, "Speed control of three phase induction motor using indirect field oriented control based on real-time control system," in *2018 10th International Conference on Information Technology and Electrical Engineering (ICITEE)*, 2018, pp. 438–442.
- [26] R. Arulmozhiyal and R. Kandiban, "Design of fuzzy PID controller for brushless DC motor," in *2012 International Conference on Computer Communication and Informatics*, 2012, pp. 1–7.
- [27] R. K. Mudi and N. R. Pal, "A self-tuning fuzzy PI controller," *Fuzzy sets Syst.*, vol. 115, no. 2, pp. 327–338, 2000.
- [28] S. Vasu, "Fuzzy PID based adaptive control on industrial robot system," *Mater. Today Proc.*, vol. 5, no. 5, pp. 13055–13060, 2018.
- [29] A. A. El-Samahy and M. A. Shamseldin, "Brushless DC motor tracking control using self-tuning fuzzy PID control and model reference adaptive control," *Ain Shams Eng. J.*, vol. 9, no. 3, pp. 341–352, 2018.
- [30] Y. Ma, Y. Liu, and C. Wang, "Design of parameters self-tuning fuzzy PID control for DC motor," in *2010 The 2nd International Conference on Industrial Mechatronics and Automation*, 2010, vol. 2, pp. 345–348.
- [31] H. Maghfiroh, A. Ramelan, and F. Adriyanto, "Fuzzy-PID in BLDC Motor Speed Control Using MATLAB/Simulink," *J. Robot. Control*, vol. 3, no. 1, pp. 8–13, 2022.